Coupled Systems Mechanics, *Vol. 6, No. 2 (2017) 127-139*
DOI: https://doi.org/10.12989/csm.2017.6.2.127

Effectiveness of classical rolling pendulum bearings

Ioannis G. Raftoyiannis* and George T. Michaltsos[a]

Department of Civil Engineering, National Technical University of Athens,
9 Iroon Polytechneiou Str., Athens 15780, Greece

(Received January 12, 2015, Revised December 11, 2015, Accepted December 21, 2015)

Abstract. During the last decades, Pendulum Bearings with one or more concave sliding surfaces have been dominating bridge structures. For bridges with relative small lengths, the use of classical pendulum bearings could be a simple and cheaper solution. This work attempts to investigate the effectiveness of such a system, and especially its behavior for the case of a seismic excitation. The results obtained have shown that the classical pendulum bearings are very effective, mainly for bridges with short or intermediate length.

Keywords: dynamics of bridges; pendulum bearings; seismic excitation

1. Introduction

Although considerable progress has been made in earthquake engineering towards the end of last century, catastrophic bridge failure examples are found wherever large-scale earthquakes occur.

In the last years, besides the use of multilayer elastomeric isolators, an alternative solution has been developed: the friction pendulum bearing systems, taking advantage of a different approach in contrast to the friction systems.

Among the structures, bridges are vulnerable when subjected to severe earthquakes. Bridge structural damages occur primarily in the piers, which may in turn result in collapse of the bridge spans. Although the ductility design concept has been widely accepted for seismic design of structures in engineering practice, this may not be appropriate for bridges since they are short of structural redundancy by nature. Nevertheless, ultimate strength design does not seem to work for bridge structures as often the piers are found to fail in shear rather than flexure. The effort on protection of bridges against earthquakes should therefore be focused on minimizing the forces to be carried by the piers, in particular the shear forces. Although rubber bearings have been extensively used in base isolation systems, sliding bearings have found more and more applications in recent years due to economical reasons.

Zayas *et al*. (1987) conducted several experimental tests on a friction pendulum (FPS) earthquake resisting system. Kawamura *et al*. (1988) studied a sliding-type base isolation system identifying its composition and element properties. Buckle and Mayes (1990) presented a review

*Corresponding author, Associate Professor, E-mail: rafto@central.ntua.gr
[a]Professor, E-mail: michalts@central.ntua.gr

http://www.techno-press.org/?journal=csm&subpage=8 ISSN: 2234-2184 (Print), 2234-2192 (Online)

on seismic isolation and performance of structures through practical applications. Constantinou *et al*. (1993) presented an experimental and analytical study of a friction pendulum system (FPS) for sliding seismic isolation systems of bridges. Kim and Yun (2007) studied the seismic response characteristics of bridges using double concave friction pendulum bearings with tri-linear behavior. Marin-Artieda *et al*. (2009) presented an experimental study of friction pendulum bearing for bridge applications. Gao and Yuan (2014) presented a seismic response analysis of cable-sliding friction pendulum bearings in curved girder bridges.

Dynamics of sliding structures is a highly non-linear problem due to friction mechanism. Analytical solutions are complicated and restricted to harmonic motions for systems with no more than two degrees of freedom under idealized conditions as shown in the works of Westermo and Udwadia (1983) and Constantinou *et al*. (1993). More realistic transient responses to isolating sliding systems can be obtained only numerically.

Many numerical tests on a rigid frame model were conducted by Mosqueda *et al*. (2004). Khoshnoudian and Hagdoust (2009) showed that the interaction between the stiffness of the two horizontal directions reduces structural shear, and that the vertical component of an earthquake considerably affect the lateral response of the bridge.

It is clear, that in the last years, the protection of bridges against earthquakes is focused on the use of rubber bearings and sliding bearings, while the old classical pendulum rolling bearings are practically abandoned. One must mention at this point the works by Guo *et al*. (2009), Madhekar and Jangid (2010) and Cheng *et al*. (2010) where viscous dampers are employed as base isolator systems in bridges. Yang *et al*. (2011) presented an experimental study with dampers on suspension bridges, while Moliner *et al*. (2012) studied the retrofit of an existing railway bridge with viscoelastic dampers. The effect of tuned mass dampers and other semi-active systems on the behavior of bridges are also presented in the works of Daniel *et al*. (2012), Maddaloni *et al*. (2013), Wu *et al*. (2014) and Casalotti *et al*. (2014).

The present work attempts to investigate the effectiveness of a classical rolling pendulum bearing (CPRB) system and especially, its behavior for the case of a seismic excitation. The CPRB solution with different forms (see Fig. 1) was described, patented and finally used by Touaillon (1870).

2. Introductory concepts

2.1 The classical pendulum rolling bearing (C.P.R.B.)

Let us consider a C.P.R.B. isolator with one concave rolling like the one shown in Fig. 1(a).

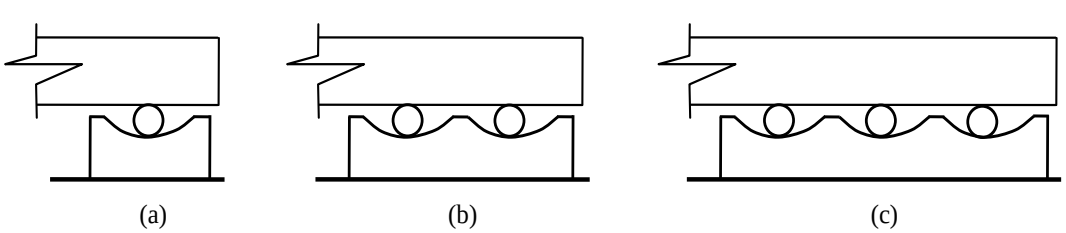

Fig. 1 The use of a CPRB with one, two and three concaves

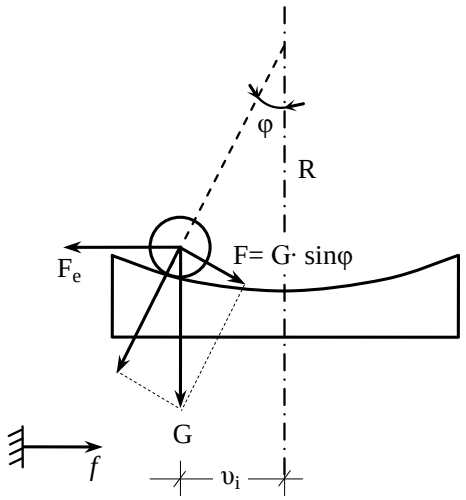

Fig. 2 Kinematics of a C.P.R.B. with one concave

For angles φ up to ~15° (0.2618 rad), which is a usual limit-value of the maximum displacement of a friction isolators, it is $\tan\varphi$-$\sin\varphi$=0.009<<1.

Therefore, one can set

$$\begin{aligned} \tan\varphi &\cong \sin\varphi \\ \cos\varphi &\cong 1 \end{aligned} \tag{1}$$

Analyzing the weight G into the components F and V, the following relation $F=G\sin\varphi$ is valid, or according to Fig. 2

$$F = G \cdot \frac{\upsilon_i}{R} \tag{2}$$

This mechanism acts as damper through the forces F (Fig. 2) that are developed because of the weight G. The friction forces, due to rolling friction, can be neglected, given that the rolling friction coefficient (for a steel ball or a cylinder rolling on steel), is up to 0.004. On the other hand, the angle of the friction cone amounts up to 0.23°, which means a very small static friction.

It is obvious that the possibilities of such bearings are limited due to their limited strength and therefore, they can be applied on bridges with total length up to 70 or 80 meters.

2.2 The bridge

Let us consider a bridge under earthquake forces but without live loads resting on F.P.B. isolators. The total lateral displacement of an arbitrary point $A(x)$ at position x along the length of the bridge is given by the following relation (see Fig. 3)

$$\upsilon(x,t) = f(t) + \upsilon_i(t) + \upsilon_o(x,t) \tag{3}$$

where $f(t)$ is the displacement of the foundation due to earthquake, $\upsilon_i(t)$ is the displacement of the bridge support from the isolator's axis, and $\upsilon_o(x,t)$ is the elastic deformation of the bridge at point $A(x)$ due to bending.

Considering for example that each edge of the bridge is based on four supports (see Fig. 3) and under condition of a non-deformable cross-section, the total acting forces are

$$\left.\begin{aligned} H &= \int_0^{\ell} m \cdot \ddot{\upsilon}\, dx\,, \\ V &= m \cdot g \cdot \ell \end{aligned}\right\} \qquad (4a,b)$$

Thus, on each extreme support V_1, it will be $V_i = \frac{m\,g\,\ell}{8}$, and since it is $V_1=3V_2$ and $V_1+V_2\cdot b/3=H\cdot e/2$, one finally has $V_1 = \frac{H\,e}{2b(1+1/9)}$.

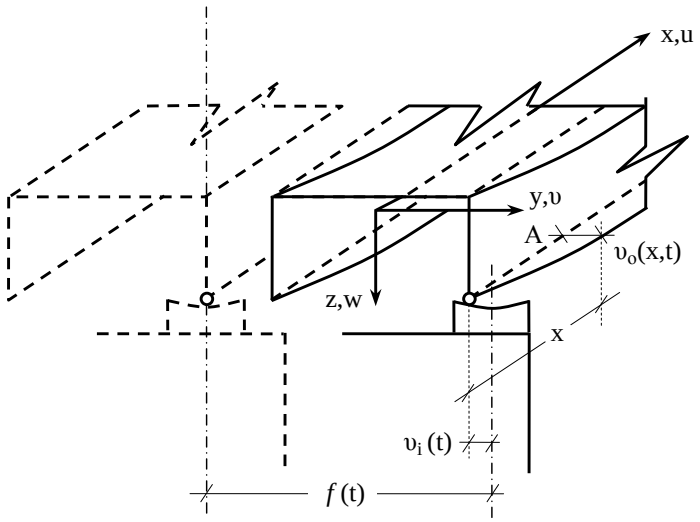

Fig. 3 Displacement of a point A on the bridge

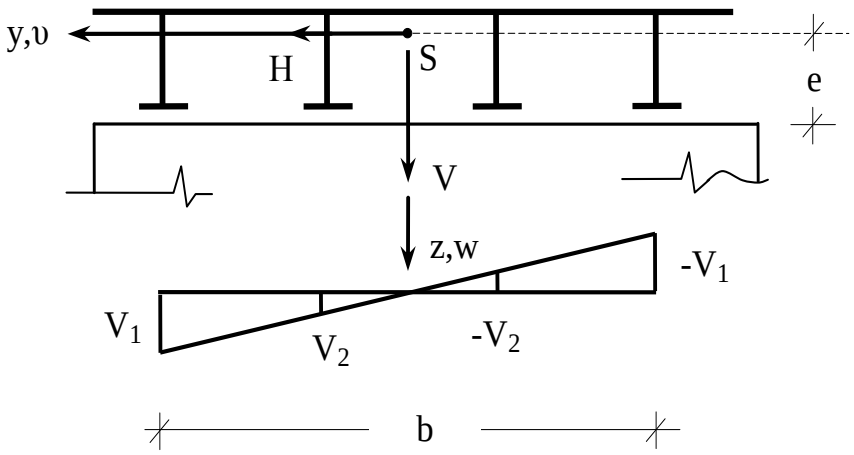

Fig. 4 Reaction forces developing at the supports

Therefore, the forces acting on Support 1 will be

$$\left.\begin{aligned} H_1 &= \frac{1}{8}\cdot\int_0^{\ell} m\ddot{\upsilon}\,dx, \\ V_1 &= \frac{mg\ell}{8} + \frac{e}{b(1+1/9)}\cdot\int_0^{\ell} m\ddot{\upsilon}\,dx \end{aligned}\right\} \tag{5a,b}$$

where *e* is the distance between the gravity center and the isolator. Similarly, for a bridge based on two isolators at each end, it will be

$$\left.\begin{aligned} H_1 &= \frac{1}{4}\cdot\int_0^{\ell} m\ddot{\upsilon}\,dx, \\ V_1 &= \frac{mg\ell}{4} + \frac{e}{2b}\cdot\int_0^{\ell} m\ddot{\upsilon}\,dx \end{aligned}\right\} \tag{6a,b}$$

3. The governing equations of motion

The divergence forces (i.e., the inertia forces caused by an earthquake) are due to the total displacement of the bridge and thus, they will be equal to

$$Fe = \int_0^{\ell} m\ddot{\upsilon}\,dx = \int_0^{\ell} m(\ddot{f} + \ddot{\upsilon}_i + \ddot{\upsilon}_o)\,dx \tag{7}$$

The above forces must be equilibrated by the restoring forces $G\upsilon_i/R$, while for values of angle $\varphi<15°$, the following equation is valid

$$\int_0^{\ell} m\ddot{\upsilon}\,dx + G\frac{\upsilon_i}{R} = 0 \tag{8a}$$

On the other hand, the equation of motion of the bridge is $EI_z\upsilon'''' + c\dot{\upsilon} + m\ddot{\upsilon} = 0$, which due to Eq. (3) becomes

$$EI_z\upsilon_o'''' + c\dot{\upsilon}_o + m\ddot{\upsilon}_o = -c\dot{f} - m\ddot{f} - c\dot{\upsilon}_i - m\ddot{\upsilon}_i \tag{8b}$$

Solution of the above system of Eqs. (8a) and (8b) gives the unknowns $\upsilon_o(x,t)$ and $\upsilon_i(t)$. The elastic displacement $\upsilon_o(x,t)$ can be expressed as follows

$$\upsilon_o(x,t) = \sum_{\rho} \Psi_\rho(x)\Phi_\rho(t) \tag{9}$$

where $\Psi_\rho(x)$ are the shape functions of the bridge for lateral displacements and $\Phi_\rho(t)$ are time functions under determination. Introducing Eq. (9) into Eqs. (8a) and (8b), because of Eq. (3), and taking into account that $\Psi_\rho(x)$ satisfy the equation of free motion, one obtains after some manipulations the following system of equations of motion

$$\left.\begin{aligned}
&\sum_{\rho}\ddot{\Phi}_{\rho}(t)\int_{0}^{\ell}\Psi_{\rho}(x)dx+\frac{g\,\ell}{R}\upsilon_{i}(t)+\ell\,\ddot{\upsilon}_{i}(t)+\ell\,\ddot{f}(t)=0\\
&\ddot{\Phi}_{\rho}+\frac{c}{m}\dot{\Phi}_{\rho}+\omega_{\rho}^{2}\Phi_{\rho}=\frac{\int_{0}^{\ell}\Psi_{\rho}dx}{\int_{0}^{\ell}\Psi_{\rho}^{2}dx}\cdot\left(-\frac{c}{m}\dot{f}-\ddot{f}-\frac{c}{m}\dot{\upsilon}_{i}-\ddot{\upsilon}_{i}\right),\quad \rho=1,\ldots,n
\end{aligned}\right\} \tag{10a,b}$$

From the above system of Eqs. (10a) and (10b), one can determine the unknown functions $\upsilon_i(t)$ and $\Phi_\rho(t)$.

4. Solution of the problem

In order to solve the above system, the Laplace transformation is employed. Thus, by setting

$$\left.\begin{aligned}
&L\Phi_{\rho}(t)=\varphi_{\rho}(p)\,,\\
&L\upsilon_{i}(t)=U_{i}(p)\,,\\
&Lf(t)=F(p)
\end{aligned}\right\} \tag{11a,b,c}$$

with initial conditions

$$\left.\Phi_{\rho}(0)=\upsilon_{i}(0)=f(0)=0\quad\right\} \tag{12a,b,c}$$

Eqs. (10a) and (10b) become as follows

$$\left.\begin{aligned}
&\sum_{\rho}p^{2}\varphi_{\rho}\int_{0}^{\ell}\Psi_{\rho}(x)dx+\frac{g\,\ell}{R}U_{i}+\ell\,p^{2}U_{i}+\ell\,p^{2}F=0\\
&\left(p^{2}+\frac{c}{m}p+\omega_{\rho}^{2}\right)\varphi_{\rho}+\frac{\int_{0}^{\ell}\Psi_{\rho}dx}{\int_{0}^{\ell}\Psi_{\rho}^{2}dx}\cdot\left(\frac{c}{m}pF+p^{2}F+\frac{c}{m}pU_{i}+p^{2}U_{i}\right)=0\\
&\text{with:}\quad \rho=1\text{ to }n
\end{aligned}\right\} \tag{13a,b}$$

Solution of the above system of Eq. (13) gives the unknowns $U_i(p)$ and $\varphi_\rho(p)$.
Therefore, it will be

$$\left.\Phi_{\rho}(t)=L^{-1}\varphi_{\rho}(p)\,,\quad \upsilon_{i}(t)=L^{-1}U_{i}(p)\quad\right\} \tag{14a,b}$$

and from the above linear system one obtains the unknowns $\varphi_\rho(p)$ and $U_i(p)$ under the form $\Phi_{\rho}(p)=\frac{N_{\rho}(p)}{Q_{\rho}(p)}$, where $N_\rho(p)$ and $Q_\rho(p)$ are polynomials with respect to p, where $Q_\rho(p)$ is of

higher order than $N_\rho(p)$. Hence, Heaviside's rule can be applied leading finally to the following expression for $\Phi_\rho(t)$: $\Phi_\rho(t) = L^{-1}\varphi_\rho(p) = L^{-1}\left(\frac{N_\rho(p)}{Q_\rho(p)}\right) = \sum_{r=1}^{\sigma} \frac{N_r(p_r)e^{p_r t}}{Q_r(p_r)}$, where p_r are the roots of the polynomial Q_r.

5. Numerical examples and discussion

5.1 The isolator

Let us consider the CPRB shown in Fig. 5, which effectiveness is under investigation. At first, one has to comply with the following geometrical characteristics and limitations:

• The diameter of the sphere (or cylinder) must be: $d>h=R(1-\cos\varphi)$, which for $\varphi<15°$ gives

$$d>0.034\ R \tag{15a}$$

• The maximum displacement υ_i must be: $\upsilon_i<R\cdot\sin\varphi$ or

$$\upsilon_i< 0.2588\ R \tag{15b}$$

• Because of CPRB strength limitations, the maximum load that can be undertaken by such a mechanism is also limited. Therefore, a CPRB may have the form of Figs. 1(a), 1(b), 1(c), etc. This last solution of a rolling ball bearing with two or more concaves was described, patented and finally used by Jules Touaillon (1870).

5.2 The bridge

Let us consider next a single-span simply supported bridge with the following data: span length L=70.0 m, mass per unit length m=1500 kg/m, and cross-sectional moment of inertia I_z=2.0 m^2.

The first three eigenfrequencies are: ω_1=10.66, ω_2=95.92, and ω_3=266.45 sec^{-1}. The bridge has a cross-section like the one shown in Fig. 3, with width b=7.5 and distance e=1.2 m. It has been found that for span lengths L>20 m, the eigenfrequencies of a bridge are affected by the radius R of the concave less than 1.5% (Westermo and Udwadia 1983).

According to Eq. (5b), one obtains the reactions V_1=15000 kN and V_2=13500 kN, which correspond to a similar distress of the supports.

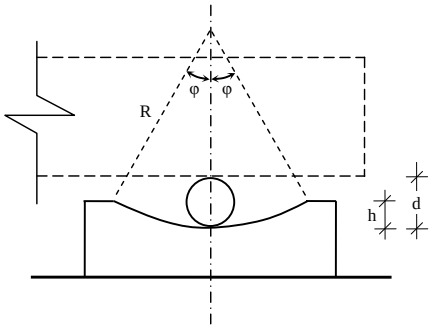

Fig. 5 A typical CPRB

5.3 The isolator's and bridge's behavior

The ground motion considered, is given by the expression $f = k \cdot e^{-\beta t} \sin \Omega t$, with k=0.05, β=0.20, and Ω=8 sec^{-1} ($\gamma \cong 3 m/sec^2$), Ω=10 sec^{-1} ($\gamma \cong 4.9 m/sec^2$), Ω=12 sec^{-1} ($\gamma \cong 6.98 m/sec^2$), where k is a constant that depends on the soil characteristics, β is the damping ratio and Ω is the frequency of the ground motions (Abrahamson *et al.* 1991), while three cases of earthquake acceleration are considered. The above ground motion is chosen as being an unfavorable one, since it corresponds to a near-source earthquake (occurring at distance less than 70 km from the bridge) and has the character of a shock.

5.3.1 Motion in parallel with ox-axis

In this case, it is υ_o=0, and the system (10a,b) reduces to the following equation

$$\ddot{\upsilon}_i(t) + (g/R) \cdot \upsilon_i(t) + \ddot{f}(t) = 0 \tag{16}$$

Applying the equations of §4, one obtains the plots of Figs. 6, 7 and 8. In these plots the displacements υ_i are drawn for various values of Ω (8, 10, 12) and R (0.6, 0.8, 1.2), respectively. Finally, in Fig. 9 the displacements υ_i are drawn for Ω=10 and various values of R (0.6, 5, 20).

It is observed that the mechanism under study is effective, absorbing the motion with small displacements even for high earthquake's accelerations (γ=7 m/sec^2).

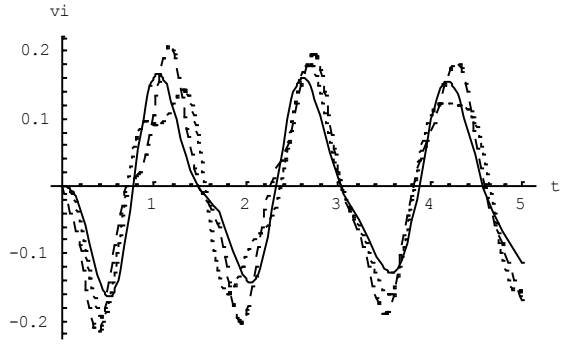

Fig. 6 The displacement υ_i for R=0.6 m and Ω=8(__), Ω=10 (_ _), Ω=12(- -) sec^{-1}

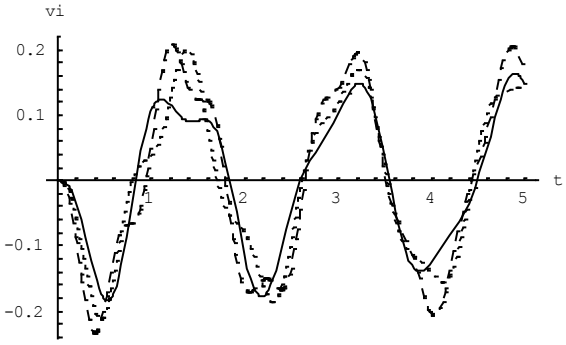

Fig. 7 The displacement υ_i for R=0.8m and Ω=8(__), Ω=10 (_ _), Ω=12(- -) sec^{-1}

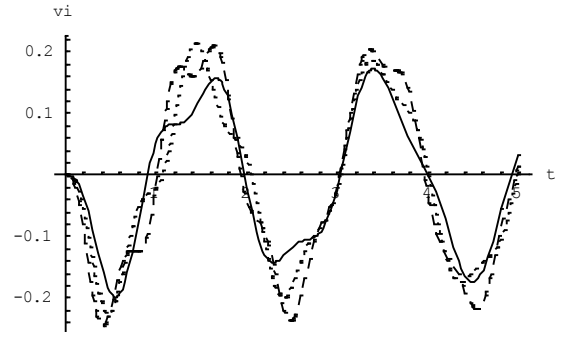

Fig. 8 The displacement υ_i for R=1.2 m and Ω=8(__), Ω=10 (_ _), Ω=12(- -) sec^{-1}

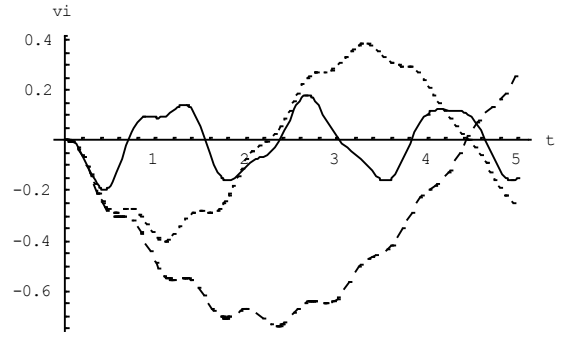

Fig. 9 The displacement υ_i for Ω=10 sec^{-1} and R=0.6 (__), R=5(- -), R=20(_ _) m

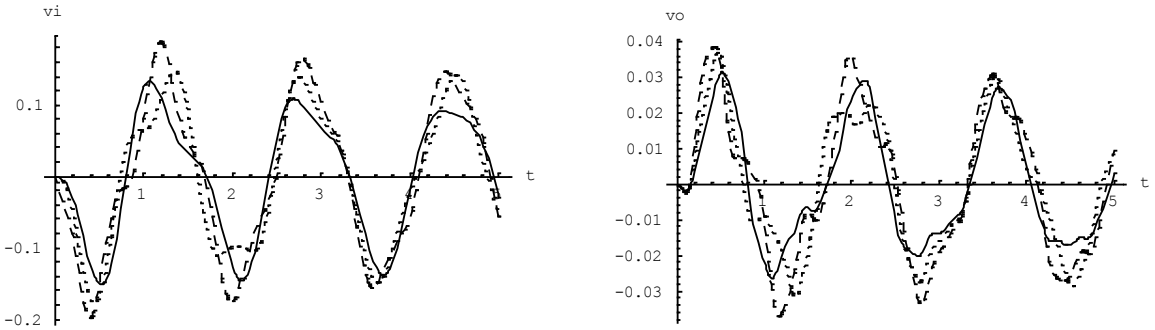

Fig. 10 The displacements υ_i and υ_o for R=0.6 m and Ω=8(__), Ω=10 (_ _), Ω=12(- -) sec^{-1}

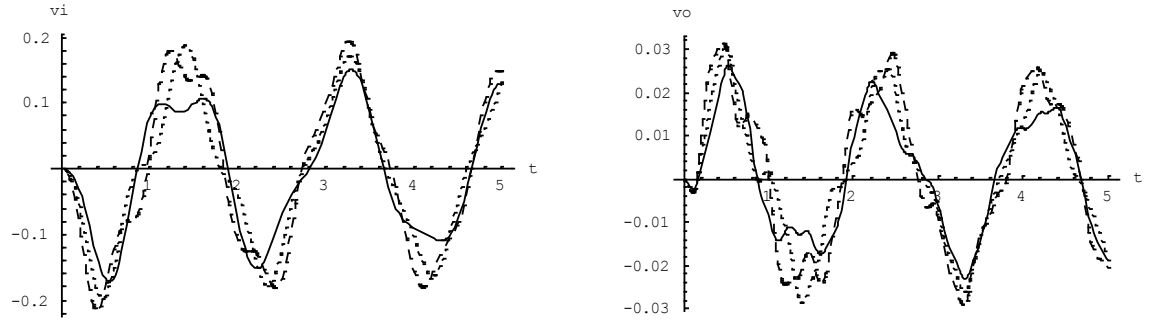

Fig. 11 The displacements υ_i and υ_o for R=0.8 m and Ω=8(__), Ω=10 (_ _), Ω=12(- -) sec^{-1}

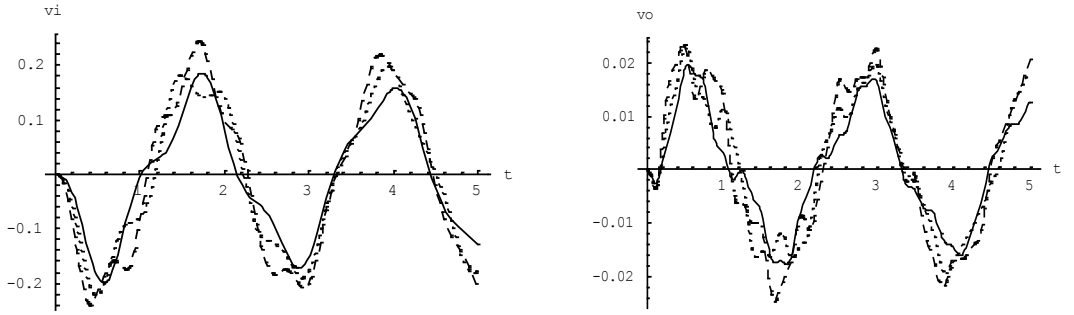

Fig. 12 The displacements υ_i and υ_o for R=1.2 m and Ω=8(__), Ω=10 (_ _), Ω=12(- -) sec^{-1}

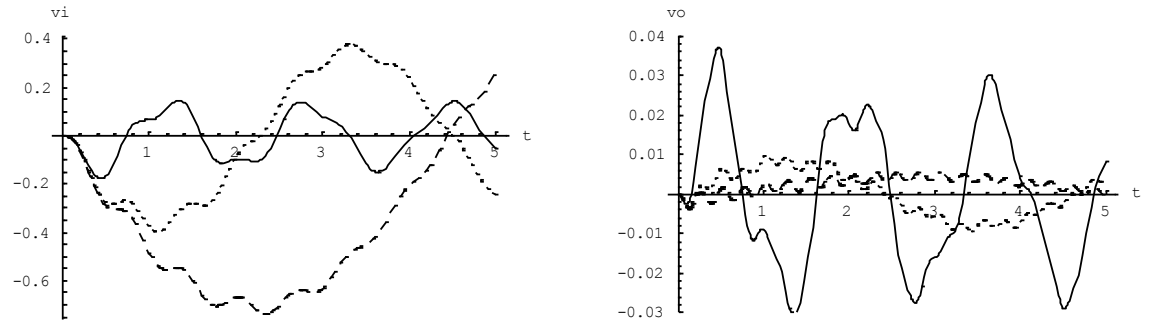

Fig. 13 The displacements υ_i and υ_o for Ω=10 sec^{-1} and R=0.6 (__), R=5(---), R=20 (_ _) m

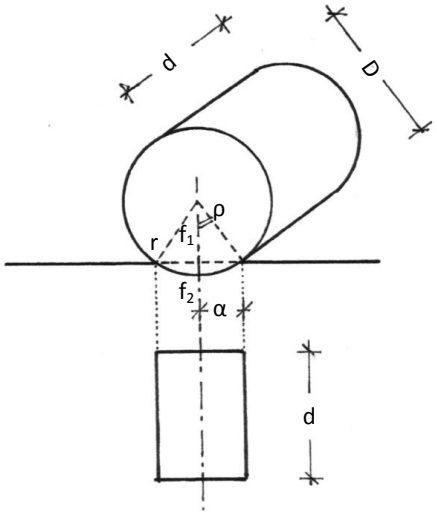

Fig. 14 Geometry of a cylindrical bearing

5.3.2 Motion in parallel with oy-axis

The plots of Figs. 10, 11, 12 and 13 show the same behavior as in the previous figures but for motion in parallel with oy-axis.

It is observed that the studied mechanism of isolators is very effective, minimizing the deformations of the bridge υ_o (υ_o=0.32 m at x=L/2 without isolators, for γ=6.9 m/sec^2). The decrease of the deformation υ_o amounts up to 93% for R=1.2 m and γ=6.9 m/sec^2 and up to 87% for R=0.6 m and γ=6.9 m/sec^2.

6. Design of a C.R.P.B. device

6.1 Bearing capacity

Manufactures of ball bearings typically publish "LOAD RATINGS" for each bearing they produce. The methods used to calculate loads, is possible to vary from manufacturer to manufacturer. However, both ABMA and ISO have published standards related to load ratings.

- ABMA std. 9-Load Ratings and Fatigue life for Ball Bearings
- ABMA std. 12.1 and 12.2-Instrument Ball Bearings
- ISO 76-Static Load Ratings
- ISO 281-Dynamic Load Ratings and Rating Life.

With regard to load ratings, one must take into account that static load ratings and dynamic load ratings are calculated on completely different ways and that there is no direct relationship to each other.

The Basic Static Load Rating applies to bearings where motion does not occur or occurs only infrequently. The basic load ratings and calculation methods are based on methods described by the above mentioned ISO recommendations.

As a standard of permissible static load, the basic load rating is specified as follows:

- Maximum contact pressure at the contact point 4200 MPa (1 MPa=100 N/cm^2).

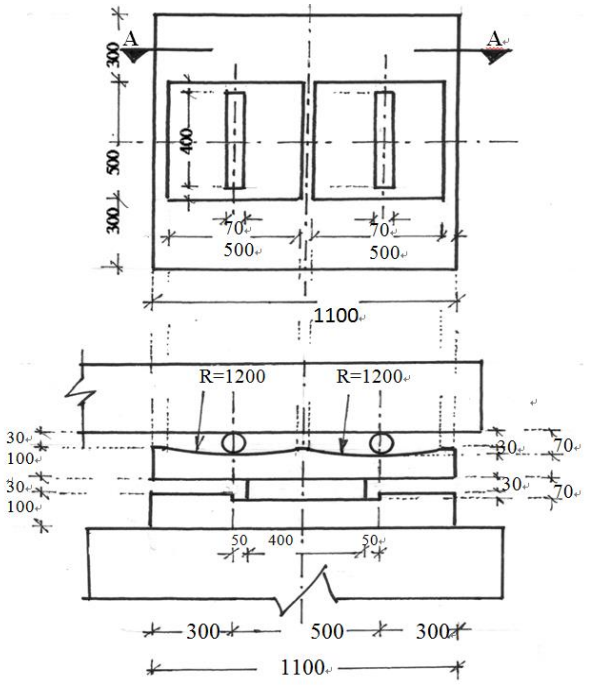

Fig. 15 The required C.R.P.B. device

• Total permanent deformation of the compressed zone can be, approximately, 1/10000th of the rolling elementary diameter.

• The basic load rating for stainless steel is 80% of that for standard bearing steel.

According to the above rules, one can get the following (see also Fig. 14): $f_2 = \dfrac{2r}{10000} = r \cdot 2 \cdot 10^{-4}$ and $f_1 = r - f_2 = 0.9998 \cdot r$

From the above, one finds: $\cos\rho = \dfrac{f_1}{r} = 0.9998 = \text{constant}$, or finally

$$\rho = 0.020\,\text{rad}\,(\sim 1.146^{o}) = \text{constant} \tag{17.1}$$

From the sketch of Fig. 14, it is obtained

$$\alpha \cong 2\pi r \frac{\rho}{2\pi} = \rho r \tag{17.2}$$

Therefore, for a safe undertaking of a load *V*, the required length *d* of the cylinder of Fig. 14, can be determined by

$$\left.\begin{aligned} d &= \frac{V}{2\alpha\sigma_{per}} \\ \text{or for stainless steel: } d &= \frac{1.25 \cdot V}{2\alpha\sigma_{per}} \end{aligned}\right\} \tag{17.3 a,b}$$

6.2 Design of the required C.R.P.B.

According to the results of §5, it is ascertained that the maximum displacements along both *Ox* and *Oy* axes are

$$\left.\begin{array}{l} \pm 0.22\text{m for R} = 0.6, \\ \pm 0.24\text{m for R} = 0.8\text{m}, \\ \pm 0.25\text{m for R} = 1.2\text{m} \end{array}\right\}$$

The distress of the supports is about 14000 kN or using four supports, one has 3500 kN for each support.

If a C.R.P.B. with R=1.2 m is chosen, one must have D>0.034*R=0.041 m while the allowed maximum displacement is: 0.2588*R=0.31 m.

Thus, a cylinder with D=7 cm is selected. From §6.one has $\alpha = \rho\, r = 0.020 \cdot 3.5 = 0.07\,\text{cm}$ and $d = \dfrac{V}{2\,\alpha\,\sigma_{per}} = \dfrac{350000}{2 \cdot 0.07 \cdot 42000} = 59.5\text{cm}$ or 2 cylinders with 40 cm length each.

The so-designed C.R.P.B. device (shown in Fig. 15) can undertake loads acting on both directions since the rolling cylinders operate along two vertical axes.

7. Conclusions

Based on the results of the CPRB model considered herein, one can draw the following conclusions:

• The CPRB systems are effective for a wide variety of earthquakes.

• For motions acting in parallel to O-*x* or O-*y* axes, the isolator's displacements come up with a magnitude from 0.15 to 0.31 rad. These last values occur for seismic accelerations higher than 6.9 m/sec^2.

• The decrease of the bridge's oscillations can be in the order of 90-95%, e.g., for γ=6 m/sec^2 it is υ_o=0.038 m when using CPRB, while it is υ_o=0.32 m without CPRB.

• As the concave radius R increases the elastic displacement υ_o decreases and the displacement υ_i of the device increases, respectively. This last displacement reaches unacceptable values for R>2 m.

References

Abrahamson, N.A., Schneider, J.F. and Stepp, J.C. (1991), "Empirical spatial coherency functions for application to soil-structures interaction analyses", *Earthq. Spec.*, **7**(1), 25-32.

Buckle, I.G. and Mayes, R.L. (1990), "Seismic isolation history: Application and performance-a world review", *Earthq. Spec.*, **6**(2), 161-201.

Casalotti, A., Arena, A. and Lacarbonara, W. (2014), "Mitigation of post-flutter oscillations in suspension bridges by hysteretic tuned mass dampers", *Eng. Struct.*, **69**, 67-71.

Cheng, S., Darivandi, N. and Ghrib, F. (2010), "The design of an optimal viscous damper for a bridge stay cable using energy-based approach", *J. Sound Vibr.*, **329**(22), 4689-4704.

Constantinou, M.C., Tsopelas, P., Kim, Y.S. and Okamoto, S. (1993), "NCEER-Taisei corporation research

program on sliding seismic isolation systems for bridges: Experimental and analytical study of a friction pendulum system (FPS)", Technical Report NCEER-93-0020, NCEER, SUNY, New York, U.S.A.
Daniel, Y., Lavan, O. and Levy, R. (2012), "Multiple-tuned mass dampers for multimodal control of pedestrian bridges", *J. Struct. Eng.*, **138**(9), 1173-1178.
Gao, K. and Yuan, W. (2014), "Seismic response analysis of cable-sliding friction pendulum bearings in curved girder bridges", *J. Earthq. Eng. Vibr.*, **34**(3), 41-66.
Guo, A., Li, Z., Li, H. and Ou, J. (2009), "Experimental and analytical study on pounding reduction of base-isolated highway bridges using MR dampers", *Earthq. Eng. Struct. Dyn.*, **38**(11), 1307-1333.
Kawamura, S., Kitazawa, K., Hisano, M. and Nagashima, I. (1988), "Study of a sliding-type base isolation system-system composition and element properties", *Proceeding of the* 9*th WCEE*, Tokyo, Kyoto, Japan.
Khoshnoudian, F. and Hagdoust, V.R. (2009), "Response of pure-friction sliding structures to three components of earthquake excitation considering variations in the coefficient of friction", *Civil Eng.*, **16**(6), 429-442.
Kim, Y.S. and Yun, C.B. (2007), "Seismic response characteristics of bridges using double concave friction pendulum bearings with tri-linear behavior", *Eng. Struct.*, **29**(11), 3082-3093.
Maddaloni, G. Caterino, N., Nestovito, G. and Occhiuzzi, A. (2013), "Use of seismic early warning information to calibrate variable dampers for structural control of a highway bridge: Evaluation of the system robustness", *Bull. Earthq. Eng.*, **11**(6), 2407-2428.
Madhekar, S.N. and Jangid, R.S. (2010), "Seismic response control of benchmark highway bridge using variable dampers", *Smart Struct. Syst.*, **6**(8), 953-974.
Marin-Artieda, C., Whittaker, A. and Constantinou, M. (2009), "Experimental study of the XY-friction pendulum bearing for bridge applications", *J. Brid. Eng.*, **14**(3), 193-202.
Moliner, E., Museros, P. and Martinez-Rodrigo, M.D. (2012), "Retrofit of existing railway bridges of short to medium spans for high-speed traffic using viscoelastic dampers", *Eng. Struct.*, **40**, 519-528.
Mosqueda, G., Wittaker, A.S. and Fenves, G.L. (2004), "Characterization and modeling of friction pendulum bearings subjected to multiple components of excitation", *J. Struct. Eng.*, **130**(3), 433-442.
Mostaghel, N., Hejazi, M. and Tanbakuchi, J. (1983), "Response of sliding structures to harmonic support motion", *Earthq. Eng. Struct. Dyn.*, **11**(3), 355-366.
Touaillon, J. (1870), *Improvement in Buildings*, U.S. Patent Office, Letters Patent No. 99973.
Yang, M.G., Chen, Z.Q. and Hua, X.G. (2011), "An experimental study on using MR damper to mitigate longitudinal seismic response of a suspension bridge", *Soil Dyn. Earthq. Eng.*, **31**(8), 1171-1181.
Westermo, B. and Udwadia, F. (1983), "Periodic response of a sliding oscillator system to harmonic excitation", *Earthq. Eng. Struct. Dyn.*, **11**(1), 135-146.
Wu, S.P., Zhang, C. and Fang, Z.Z. (2014), "Design schemes and parameter regression analysis of viscous dampers for cable-stayed bridge", *Brid. Constr.*, **44**(5), 21-26.
Zayas, V., Low, S.S. and Main, S.A. (1987), "The FPS earthquake resisting system, experimental report", Report No. UCB'EERC-87/01, Earthquake Engineering Research Center, University of California, California, U.S.A.

CC